Front. Optoelectron. 2014, 7(1): 69–73
DOI 10.1007/s12200-013-0375-1

RESEARCH ARTICLE

Simulation analysis of combined UV/blue photodetector in CMOS process by technology computer-aided design

Changping CHEN[1], Xiangliang JIN (✉)[1], Lizhen TANG[1], Hongjiao YANG[1], Jun LUO (✉)[2]

1 Faculty of Materials, Optoelectronics and Physics, Xiangtan University, Xiangtan 411105, China
2 Department of Precision Mechanical Engineering, Shanghai University, Shanghai 200444, China

© Higher Education Press and Springer-Verlag Berlin Heidelberg 2013

Abstract A composite ultraviolet (UV)/blue photodetector structure has been proposed, which is composed of P-type silicon substrate, P_{well}, N_{well} and N-channel metal-oxide-semiconductor field-effect transistor (NMOSFET) realized in the P_{well}. In this photodetector, lateral ring-shaped P_{well}-N_{well} junction was used to separate the photogenerated carriers, and non-equilibrium excess hole was injected to the P_{well} bulk for changing the bulk potential and shifting the NMOSFET's threshold voltage as well as the output drain current. By technology computer-aided design (TCAD) device, simulation and analysis of this proposed photodetector were carried out. Simulation results show that the combined photodetector has enhanced responsivity to UV/blue spectrum. Moreover, it exhibits very high sensitivity to weak and especially ultral-weak optical light. A sensitivity of 7000 A/W was obtained when an incident optical power of 0.01 μW was illuminated to the photodetector, which is 35000 times higher than the responsivity of a conventional silicon-based UV photodiode (usually is about 0.2 A/W). As a result, this proposed combined photodetector has great potential values for UV applications.

Keywords ultraviolet (UV)/blue photodetector, weak light detection, complimentary metal-oxide-semiconductor (CMOS), technology computer-aided design (TCAD)

1 Introduction

Ultraviolet (UV) detection technology is developed after infrared and laser detection technology, UV detectors are hotly researched and used in many application areas, such as environmental monitoring [1], biochemical analysis [2], and so on. Photodiodes for UV detection are required to be sensitive to blue/UV radiation but blind to visible and near-infrared radiation. Different structures have been reported to realize UV silicon photodetectors. Pauchard et al. [3] and Ghazi et al. [4] proposed the silicon based UV photodiodes fabricated in standard complimentary metal-oxide-semiconductor (CMOS) process. The first UV avalanche photodiode in CMOS technology was presented by Pauchard et al. [5], and a responsivity of about 2.3 A/W at 400 nm was achieved for a reverse bias of 19.1 V. In recent years, the development of phototransistors with high responsivity for the UV/blue spectral has attracted much interest [6–9].

Technology computer-aided design (TCAD) today becomes an extremely important research and development activity in the semiconductor industry. A modern integrated circuit cannot be developed without the massive using of computer aided design (CAD) in any step of the complex flow from an idea to final product. The development of a new CMOS process might involve nine lithography steps, six ion implantations and several diffusion, annealing, and oxidation steps. As a result, the development of new semiconductor technologies and novel semiconductor device structures has been traditionally guided by an experimental approach. The TCAD tools are chosen to analyze semiconductor devices and circuits [10–13].

In this paper, a new combined photodetector with enhanced sensitivity to UV/blue and ultral-weak optical light was proposed, and its operating principle is explained briefly in Section 2. Silvaco TCAD simulation approach is adopted in Section 3 to build the device structure and analyze its photoelectric characteristics. A structure created by Silvaco Athena tool is used for further device simulation. Variations of bulk potential, threshold voltage, output characteristics, optical response characteristics and director current (DC) characteristics before and after illuminations are simulated and analyzed respectively,

Received August 25, 2013; accepted September 30, 2013

E-mail: jinxl@xtu.edu.cn, luojun@shu.edu.cn

and the results have been obtained. Some conclusions are given in Section 4.

2 Structure and operating principle

The device structure of the combined photodetector in this paper is shown in Fig. 1(a), which consists of a N-channel metal-oxide-semiconductor field-effect transistor (NMOSFET) and a lateral photodiode. For the NMOSFET, the N^+ source is placed in the center with ring-shaped poly-silicon gate and N^+ drain. For the photodiode, the P_{well} (B, bulk) is enclosed by the ring-shaped N_{well} (C, cathode) and they form the lateral PN junction. As shown in Fig. 1(b), the proposed combined photodetector also can be realized by integrating a P-channel metal-oxide-semiconductor fiel-effect transistor (PMOSFET) and a lateral photodiode. For the PMOSFET, the P^+ source is placed in the center with ring-shaped poly-silicon gate and P^+ drain. The N_{well} (B, bulk) is surrounded by the ring-shaped P_{well} (A, anode). In brief, only the combined photodetector with NMOSFET is introduced and analyzed in this paper.

The operating principle of this combined photodetector is different from a conventional metal-oxide-semiconductor fiel-effect transistor (MOSFET). The P_{well} bulk is set to be floating, and the lateral P_{well}/N_{well} junction is used to separate photogenerated electron-hole pairs [14]. The photogenerated carriers drifting into the bulk from the space charge region formed by the lateral P_{well}/N_{well} junction would change the P_{well} bulk potential, and further more change the threshold voltage as well as the output drain current. The main purpose to design this combined photodetector with a ring-shaped structure is to enhance its sensitivity to UV/blue spectrum, because the UV photogenerated carriers are very close to the surface (within 150 nm) for the UV/blue incident light. The depletion region of the lateral P_{well}/N_{well} photodiode near the silicon surface is enlarged using the proposed ring-shaped layout. Much more photogenerated carriers would drift into the P_{well} bulk and cause a larger shift amount of the threshold voltage, which would obtain a larger photocurrent.

3 TCAD simulation and analysis

For the TCAD simulations, a device structure is defined by Athena. The doping concentration of the P_{sub} is $1 \times 10^{14}/cm^3$ for initiation. Both of the implant doses of the P_{well} and N_{well} is $8 \times 10^{12}/cm^2$ with a diffusion time of 150 min and a diffusion temperature of 1100°C. The implanted dose of the threshold voltage adjusting is $9 \times 10^{12}/cm^2$ with energy of 10 keV. For the implantation of low doping drain (LDD), the implanted dose is $3 \times 10^{13}/cm^2$ with energy of 20 keV. For the implantation of source, drain and N^+ cathode, the dose is set with energy of 50 keV, a diffusion time of 1 min and a diffusion temperature of 900°C. The complete structure for simulations is obtained after aluminum deposition and structure mirror, as shown in Fig. 2.

Photoelectric characteristics of the proposed composite photodetector are simulated and analyzed, including the illumination effects on the P_{well} bulk potential, the threshold voltage of the NMOSFET, the output characteristics of the NMOSFET, the spectral response characteristics, and the DC response characteristics.

3.1 Bulk potential

As mentioned above, photogenerated carrier holes are injected to the P_{well} bulk, whose potential is changed when the ring-shaped side P_{well}/N_{well} junction is illuminated. Under bias conditions, the P_{well} bulk is left floating and no voltage is applied to both of source and drain electrodes. A small voltage of 0.5 V is applied to the gate, and a positive voltage of 3 V is fixed to the cathode electrode. Potential variation of the P_{well} bulk is analyzed by changing the intensity of incident optical power illuminated to the photodetector. It can be seen from Fig. 3, the stronger incident optical power is, the larger change of P_{well} bulk potential is, because the amount of injected carrier holes is proportional to the intensity of incident optical power. The P_{well} bulk potential varies from negative to positive.

3.2 Threshold voltage

Changes of the P_{well} bulk potential will ultimately affect

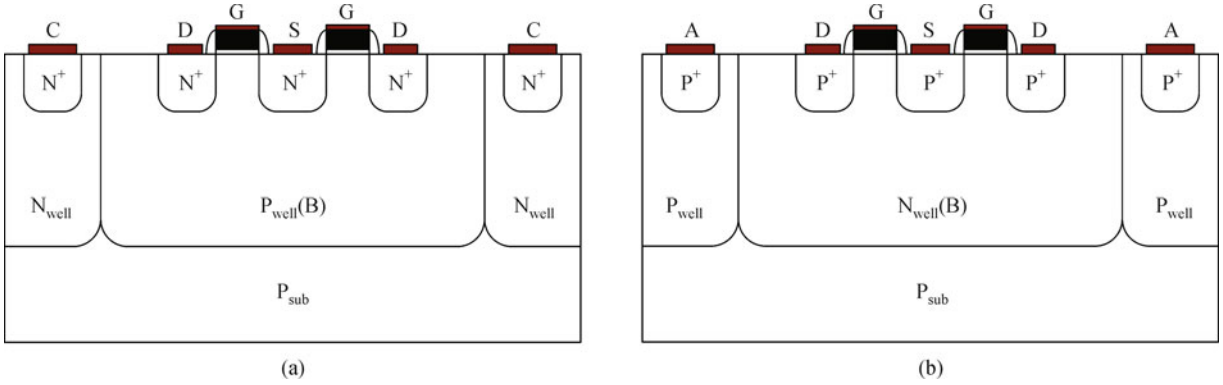

Fig. 1 Combined photodetectors with (a) NMOSFET and (b) PMOSFET

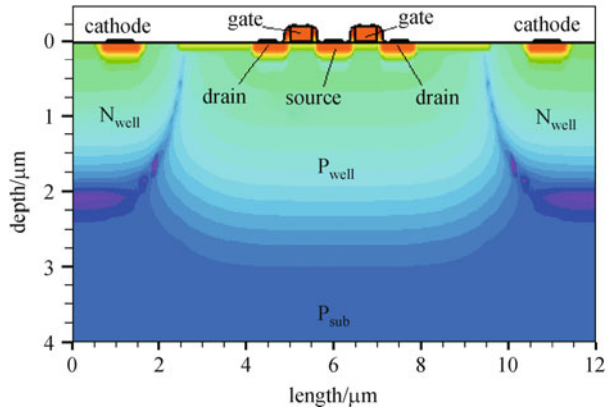

Fig. 2 Simulated structure of proposed combined photodetector for TCAD device simulation

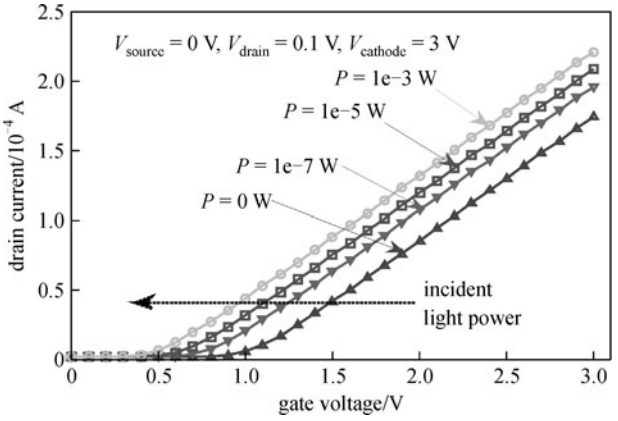

Fig. 4 Simulated threshold voltage variations with different light intensity illuminations

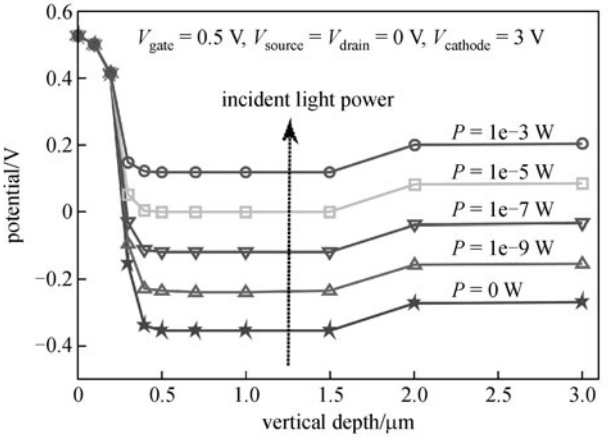

Fig. 3 Simulated variation of bulk (P_{well}) potential under different illuminations

the threshold voltage of the NMOSFET. Conclusion can be obtained from mathematical derivation that the injected carrier holes will cause a decrease to the threshold voltage. Simulation under a certain bias voltage conditions (V_{source} = 0 V, V_{drain} = 0.1 V, $V_{cathode}$ = 3 V) is conducted to testify the variation of threshold voltage. Different intensities of the incident optical power are chosen and the gate voltage is swept from 0 to 3 V to observe the conduction situation of the device, as shown in Fig. 4.

Figure 4 shows that the threshold voltage decreases after illumination, and the stronger incident optical power is, the smaller threshold voltage of the NMOSFET is, which is consistent to the theoretical derivation and interpretation.

3.3 Output characteristics

Drain current of the NMOSFET in the composite photodetector under illumination is also simulated. The source is grounded and the cathode is fixed at a bias voltage of 3 V. The drain voltage is sweeping from 0 to 3 V as the gate voltage is stepped from 0 to 3 V. As shown in Fig. 5, the drain current is zero whether the device is in an illumination or dark conditions if the gate voltage is fixed at 0 V. When the gate voltage reaches the threshold voltage of the NMOSFET, the drain current significantly increases. And the difference between the drain currents with and without illuminations becomes bigger when the gate voltage is larger. In other words, the drain current affected by light illumination is more obvious.

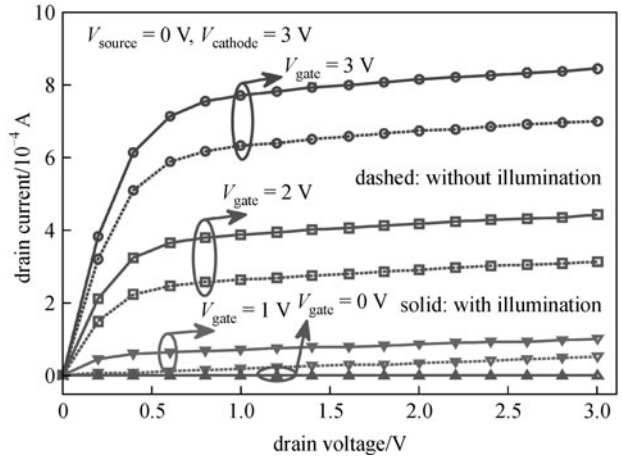

Fig. 5 Drain currents of NMOSFET with and without illuminations under different gate voltages

To investigate the effect of channel length on the optical characteristics of the device, three kinds of structures with different channel length are built and simulated respectively. The channel lengths are 0.5, 1.0 and 2.0 μm separately. Likewise, the output characteristics of each structure are also studied. In brief, only the situation that V_{gate} = 3 V is considered here in order to facilitate the analysis, and the simulated results are shown in Fig. 6. For the structure with channel length of 0.5 μm, its drain

current gets both the fastest increase, and the maximum drain current increment caused by light illumination. On the contrary, for the structure with channel length of 2.0 μm, its drain current has both the slowest increase and the minimum drain current increment caused by light illumination as shown in Fig. 7 (Noting that the drain current increment is the photocurrent of the proposed photodetedtor in this paper).

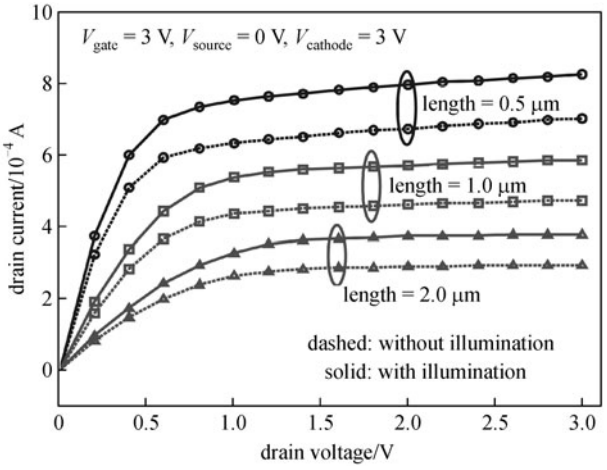

Fig. 6 Output characteristics of NMOSFET with different channel lengths

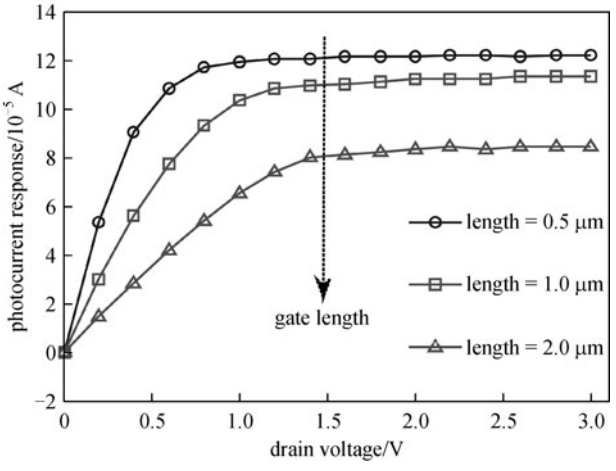

Fig. 7 Increment of drain currents after illumination for three kinds of NMOSFET structures with different channel lengths

3.4 Optical response characteristics

Spectral response characteristic of the proposed combined photodetector is studied. Bias voltage conditions here are set as follows: the source is ground; the gate, the drain and the cathode are applied with a voltage of 3 V at the same time. Simulated results are shown in Fig. 8. The drain current of the NMOSFET is almost as same as that for short lights with wavelengths less than 600 nm. When the illuminated wavelength is longer than 600 nm, the drain currents begin to decrease. As a result, it is seen that the optical response characteristic for UV/blue light is better than those for visible/infrared light (wavelength longer than 700 nm). This new combined photodetector shows enhanced UV responsivity compared to conventional silicon-based UV photodiode, whose main drawback is poor UV responsivity.

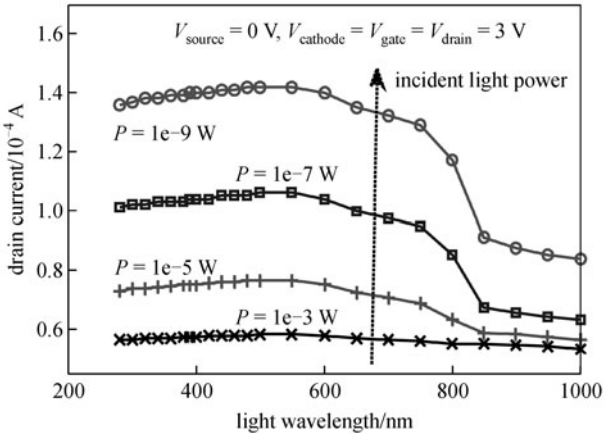

Fig. 8 Drain currents vs. wavelength with different incident light illuminations

3.5 DC response characteristics

As Section 2 described, the photocurrent response is the difference of two output drain currents of the NMOSFET that with and without illumination, respectively. And the photocurrent response divided by illumination intensity gives the DC responsivity. The DC response curves are shown in Fig. 9. The DC response is very small when the device is not applied with gate voltage, and it increases significantly if the gate voltage is fixed at a certain bias such as 1 V. The value of the DC response is almost the same size when the gate bias is 2 and 3 V respectively. These results show that the larger the intensity of incident optical power is, the smaller DC response of the device is. The DC responsivity increases rapidly if the intensity of incident optical power is smaller than a certain value. For example, when the gate voltage is 3 V and the incident power intensity is 0.01 μW, the device obtains a DC responsivity of 7000 A/W. The responsivity increases by 35000 times compared to a traditional silicon-based UV photodiode, whose responsivity is about 0.2 A/W. Therefore, the proposed combined photodetector has high potential application in ultral-weak light detections.

4 Conclusions

In this paper, a combined photodetector with enhanced sensitivity to UV/blue and ultral-weak spectrum is

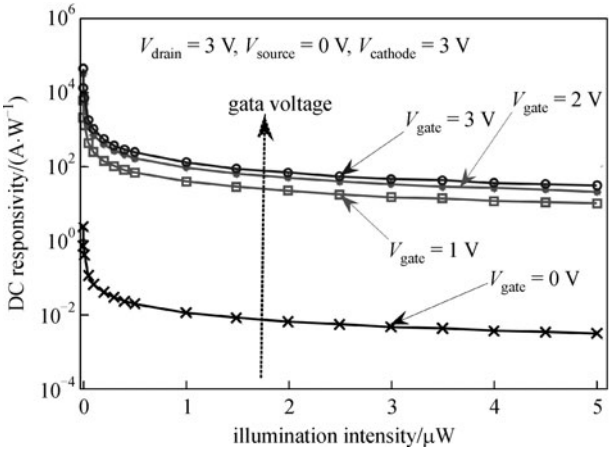

Fig. 9 DC responsivity of proposed combined photodetector with different gate voltages

proposed. TCAD approach is used to analyze its photoelectric characteristics. This new combined photodetector shows enhanced UV responsivity compared to a conventional silicon-based UV photodiode. And the spectral response characteristic for UV/blue light is better than those for visible and infrared light (wavelength longer than 700 nm). The responsivity increases by five magnitudes compared to a traditional silicon-based UV photodiode, whose responsivity is about 0.2 A/W. What's more, the proposed combined photodetector has high potential application in ultral-weak light detections.

Acknowledgements This work was supported by the State Key Program of National Natural Science of China (Grant No. 61233010), the National Natural Science Foundation of China (Grant No. 61274043), and the Program for New Century Excellent Talents in University of Ministry of Education of China (NCET-11-0975).

References

1. Charbon E. Towards large scale CMOS single-photon detector arrays for lab-on-chip applications. Journal of Physics D, Applied Physics, 2008, 41(9): 094010
2. Chang Y W, Yu P C, Huang Y T, YANG Y S. A CMOS-compatible optical biosensing system based on visible absorption spectroscopy. In: Proceedings of IEEE International Conference on Electron Devices and Solid-State Circuits. Tainan: IEEE, 2007, 1099–1102
3. Pauchard A, Besse P A, Popovic R S. A silicon blue/UV selective stripe-shaped photodiode. Sensors and Actuators A: Physical, 1999, 76(1–3): 172–177
4. Ghazi A, Zimmermann H, Seegebrecht P. CMOS photodiode with enhanced responsivity for the UV/blue spectral range. IEEE Transactions on Electron Devices, 2002, 49(7): 1124–1128
5. Pauchard A, Rochas A, Randjelovic Z, Besse P A, Popovic R S. Ultraviolet avalanche photodiode in CMOS technology. In: Proceedings of Electron Devices Meeting, IEDM'00. San Francisco, CA: IEEE, 2000, 709–712
6. Marwick M A, Andreou A G. A UV photodetector with internal gain fabricated in silicon on sapphire CMOS. In: Proceedings of Sensors 2007 IEEE. Atlanta, GA: IEEE, 2007, 535–538
7. Li G K, Feng P, Wu N J. A novel monolithic ultraviolet image sensor based on a standard CMOS process. Journal of Semiconductors, 2011, 32(10): 105008-1–105008-6
8. Weng W Y, Hsueh T J, Chang S S, Wang S B, Hsueh H T, Huang G J. A high-responsivity GaN nanowire UV photodetector. IEEE Journal of Selected Topics in Quantum Electronics, 2011, 17(4): 996–1001
9. Esmaeili-Rad M R, Papadopoulos N P, Bauza M, Nathan A, Wong W S. Blue-light-sensitive phototransistor for indirect X-ray image sensors. Electron Device Letters, 2012, 33(4): 567–569
10. Serra N, Giacomini G, Melchiorri M, Piazza A, Piemonte C, Tarolli A, Zorzi N. TCAD simulation of avalanche breakdown voltage in GM-APDs. In: Proceedings of Nuclear Science Symposium Conference Record (NSS/MIC). Knoxville, TN: IEEE, 2010, 253–259
11. Serra N, Giacomini G, Piazza A, Piemonte C, Tarolli A, Zorzi N. Experimental and TCAD study of breakdown voltage temperature behavior in n +/p SiPMs. IEEE Transactions on Nuclear Science, 2011, 58(3): 1233–1240
12. Xie F, Lu H, Chen D J, Xiu X Q, Zhao H, Zhang R, Zheng Y D. Metal-semiconductor-metal ultraviolet avalanche photodiodes fabricated on bulk GaN substrate. Electron Device Letters, 2011, 32(9): 1260–1262
13. Jacob B, Klemenc M, Petit C, Witzig A, Fichtner W. TCAD simulation of photodetector spectral response. In: Proceedings of IEEE/LEOS 3rd International Conference on Numerical Simulation of Semiconductor Optoelectronic Devices. Tokyo: IEEE, 2003, 19–20
14. Schanz M, Brockherde W, Hauschild R, Hosticka B J, Teuner A. CMOS photosensor arrays with on-chip signal processing. In: Proceedings of European Solid State Circuits Conference. Southampton UK: IEEE, 1997, 236–239